

Using New Technologies to Define the Atomic-level Details of Surface Proteins Likely to be Vaccine Targets

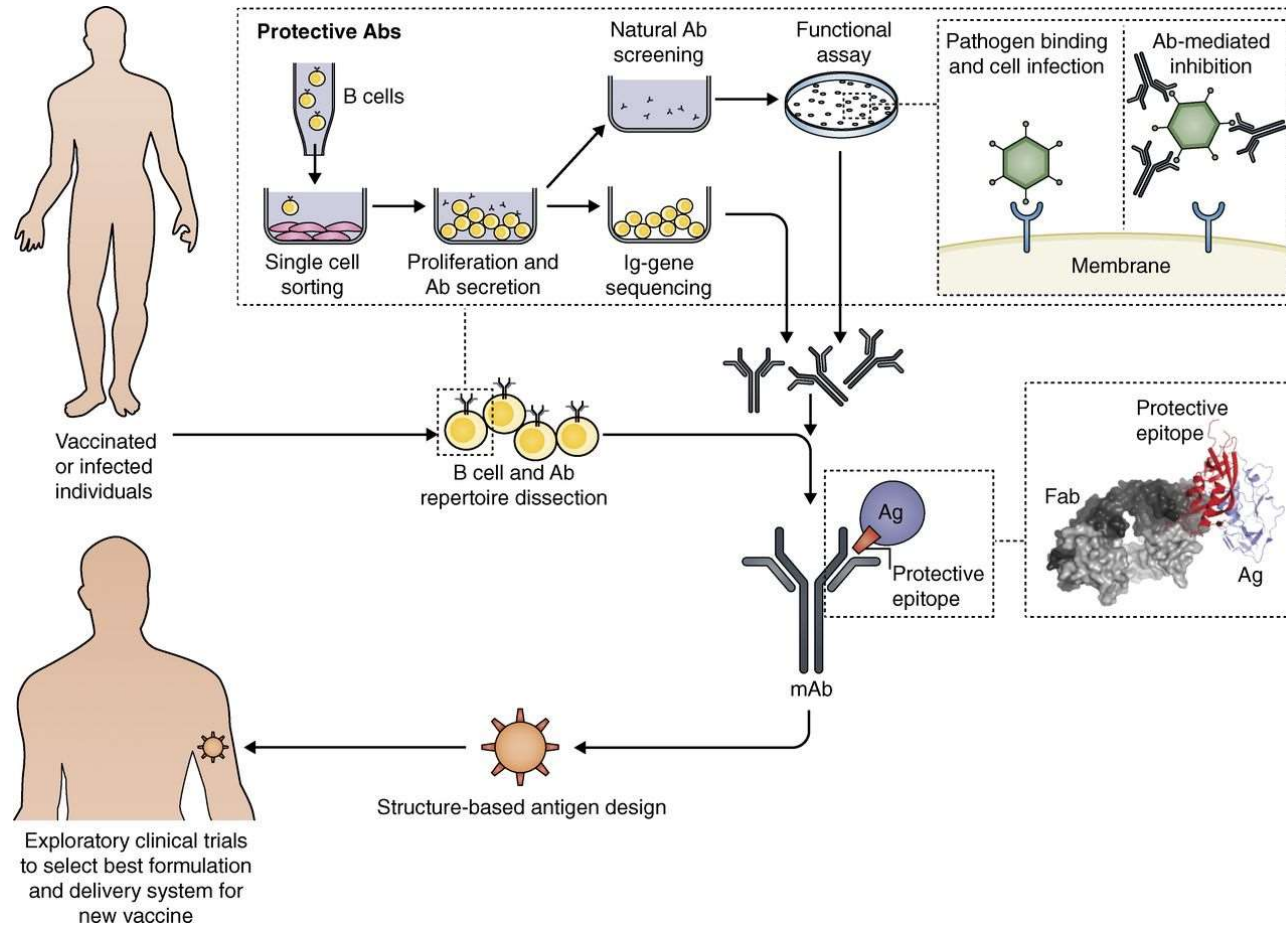
mclellanlab.org

[@mclellan_lab](https://twitter.com/mclellan_lab)

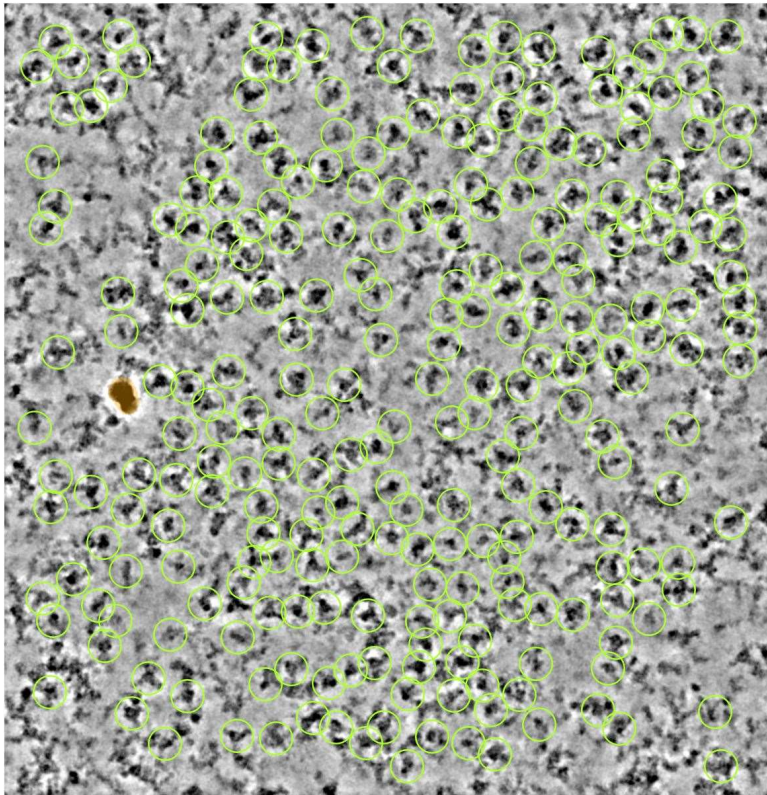
Jason S. McLellan
Department of Molecular Biosciences
The University of Texas at Austin

WHO
January 9th, 2024

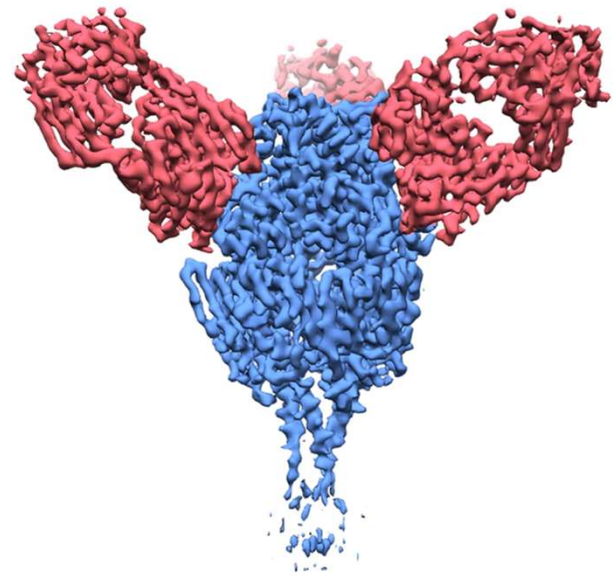
Structure-based Vaccine Antigen Design



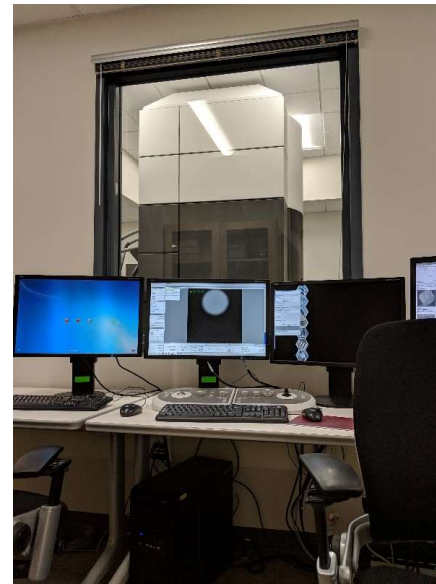
Structural Biology: Cryo-EM



10043 picks	18507 picks	17479 picks	16461 picks	15950 picks	15941 picks	15388 picks
5.0 Å 1-ess	6.0 Å 1-ess	6.0 Å 1-ess	6.0 Å 1-ess	5.9 Å 1-ess	6.0 Å 1-ess	6.0 Å 1-ess
13751 picks	13330 picks	13132 picks	13057 picks	12421 picks	12201 picks	10417 picks
6.0 Å 1-ess	6.1 Å 1-ess	6.0 Å 1-ess	6.0 Å 1-ess	6.0 Å 1-ess	6.0 Å 1-ess	6.2 Å 1-ess

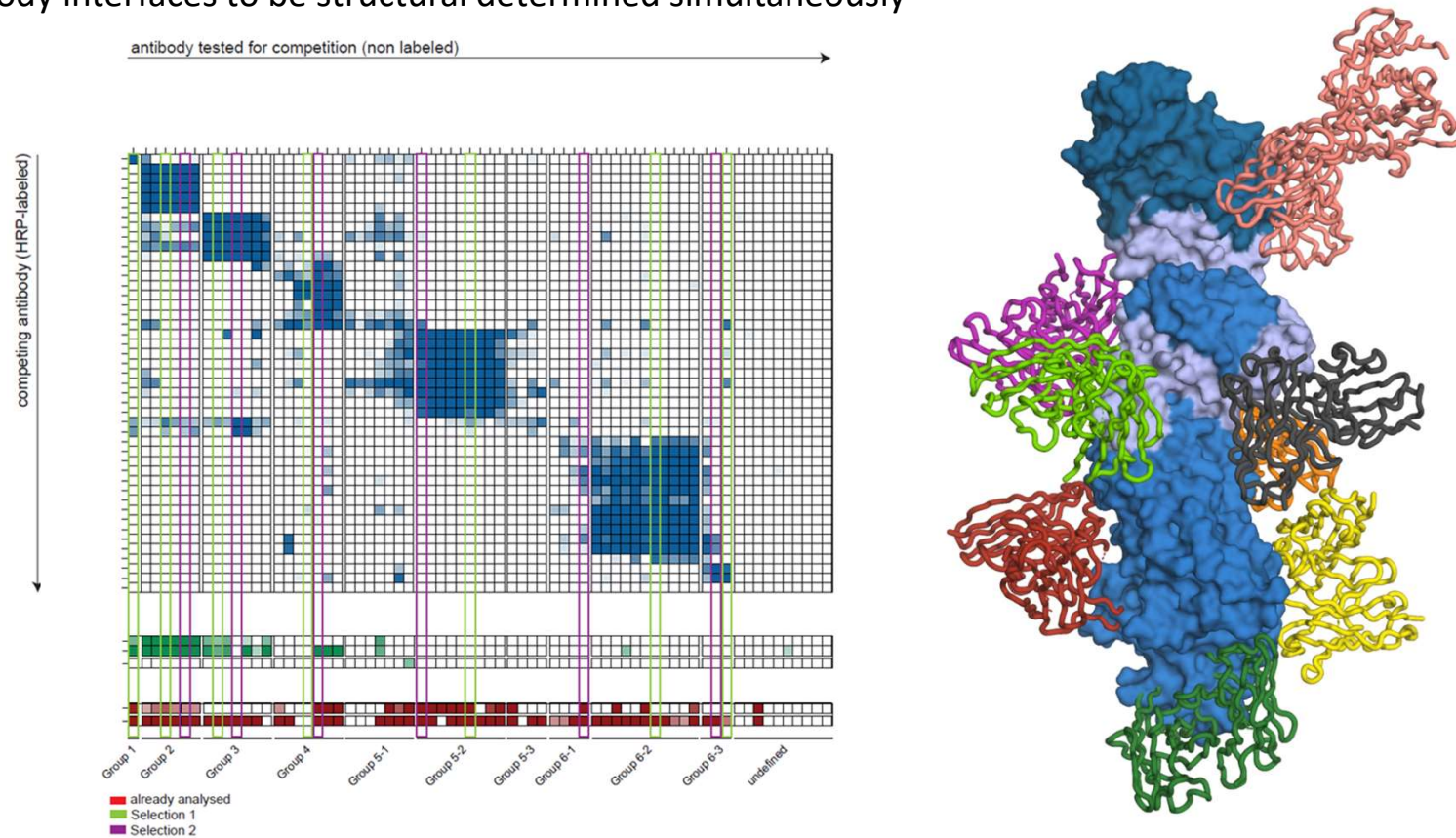


Structural Biology: Cryo-EM

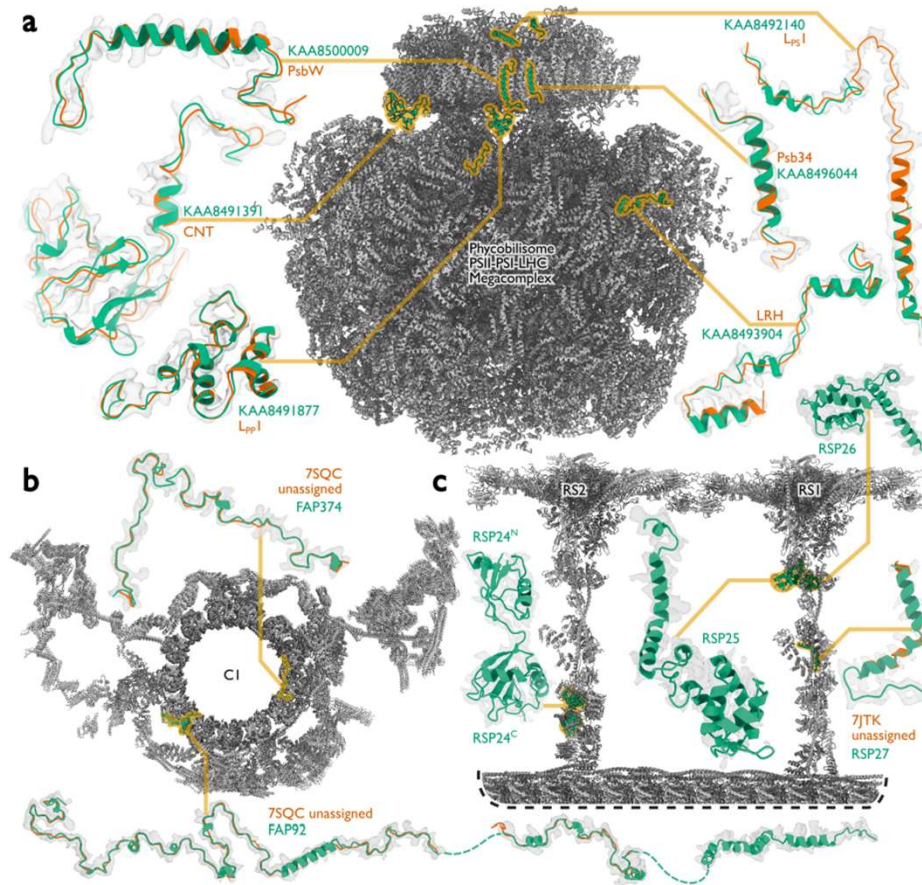
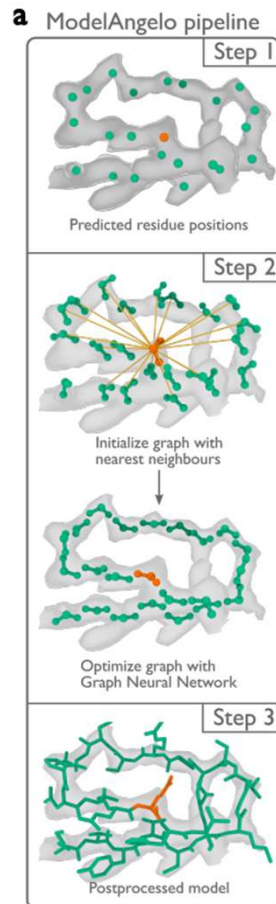


Multiplexing to Increase Antigen-Antibody Structure Throughput

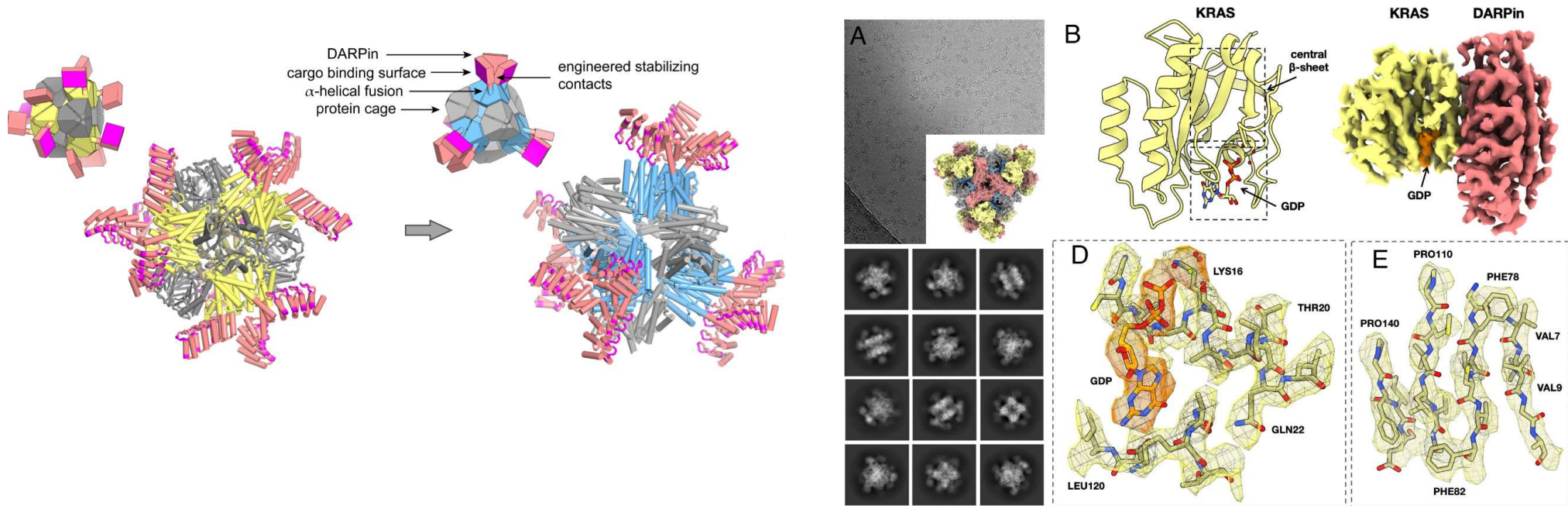
- High-throughput antibody isolation combined with precise binning of antibodies into competition groups allows multiple antibody interfaces to be structural determined simultaneously



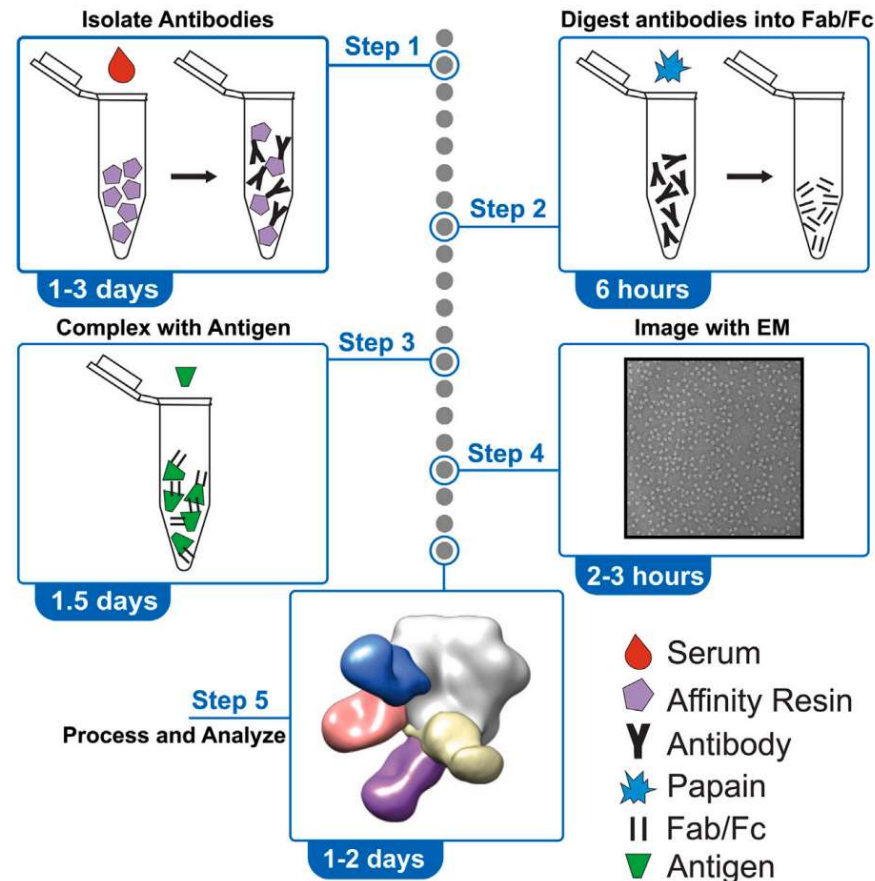
New Advances in Automated Model Building Accelerate Structure Determination Efforts



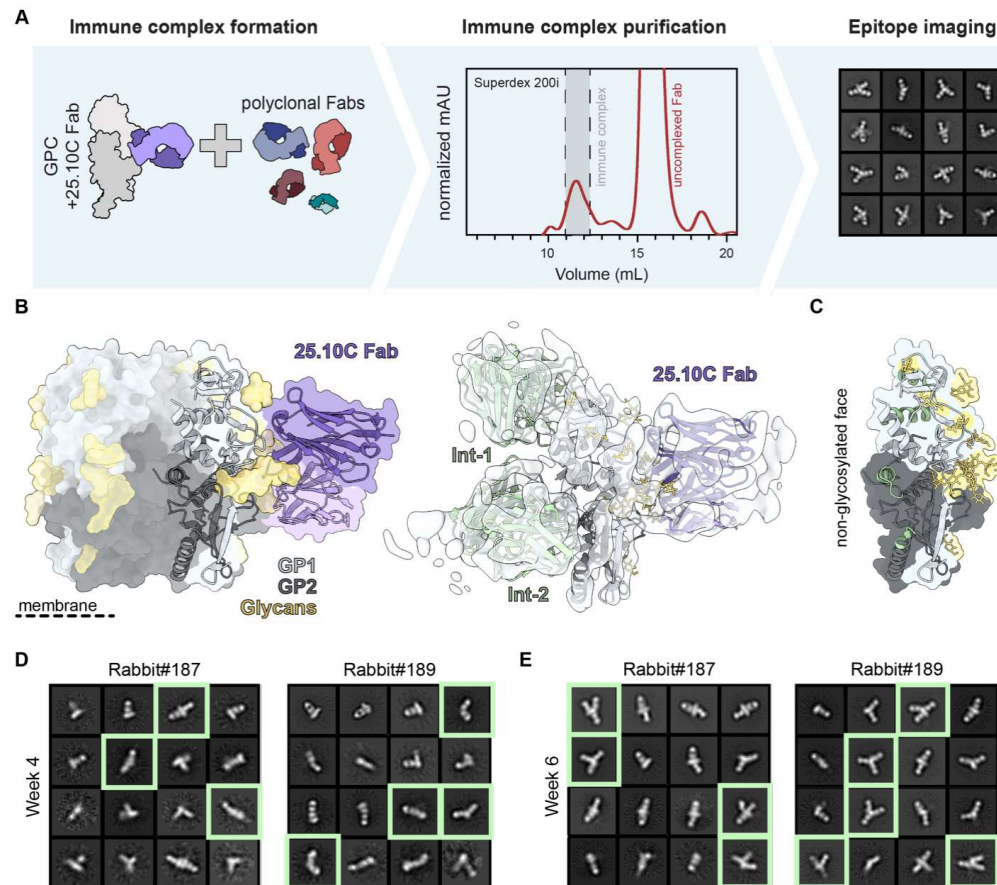
Cryo-EM Imaging Scaffolds to Enable Determination of Small Proteins



Electron-microscopy-based Polyclonal Epitope Mapping (EMPEM)

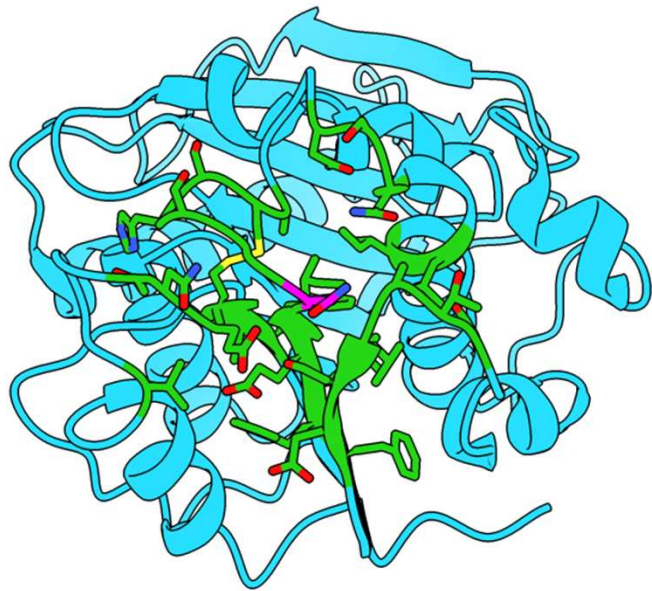


EMPEM Experiments with LASV GP Monomers Reveal Responses Targeting the Trimer Interior

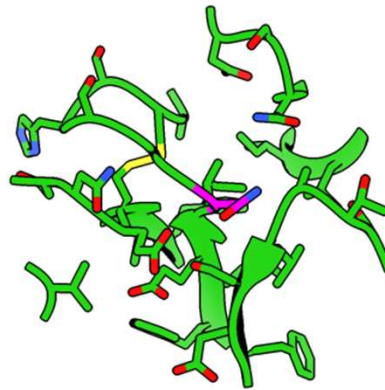


MutComputeX: Using Self-supervision to Learn What Proteins “Should” Look Like

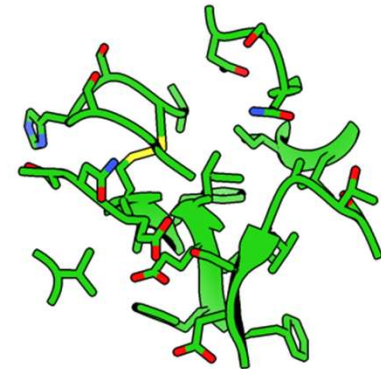
- Vision-based approach: uses protein structures for input and training



Center **microenvironment**
around an **amino acid**



Delete **remaining** protein atoms

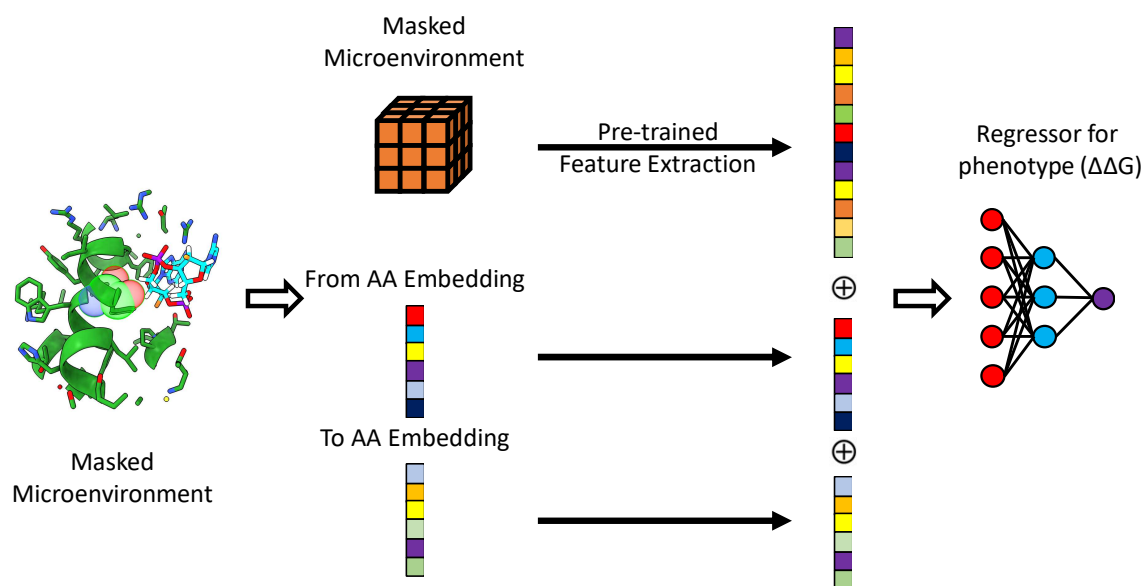


Masked Microenvironment

Delete centered **amino acid** and
use as **label**
Classification into amino acid
likelihoods

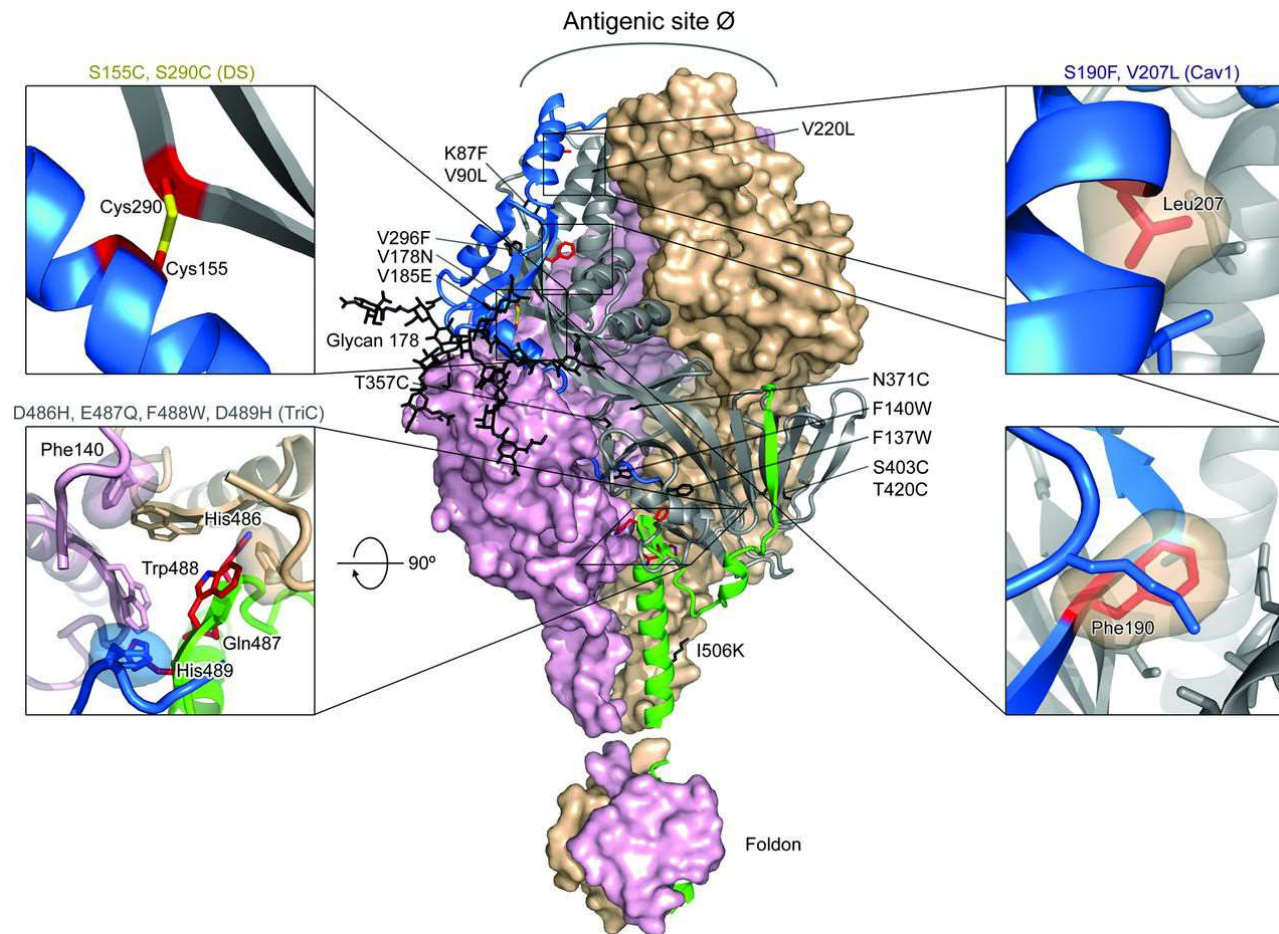
Tornøge and Altman, BMC Bioinformatics 2017

Stability Oracle: Fine-Tuning MutComputeX on Thermodynamic Stability ($\Delta\Delta G$)

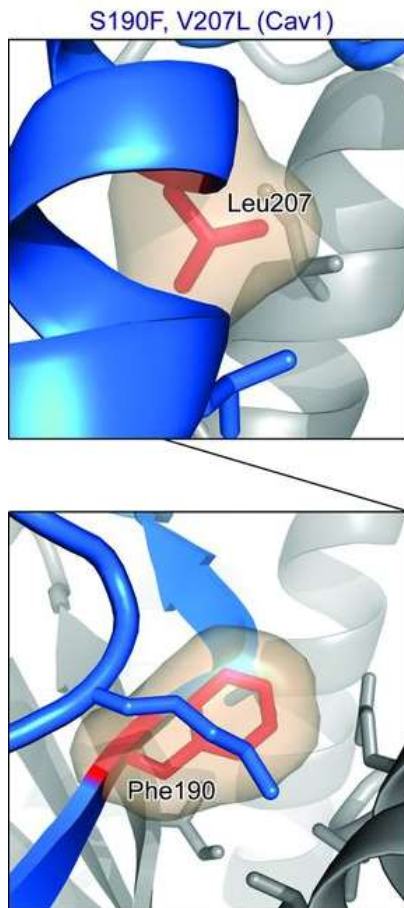


Input: Masked Microenvironment of Chemistry and vector representations of amino acids (embeddings)
Feature Extractor and **Amino Acid embeddings** are obtained from a pre-trained classification model (MutComputeX)

Stabilizing RSV Fusion (F) Glycoprotein Substitutions



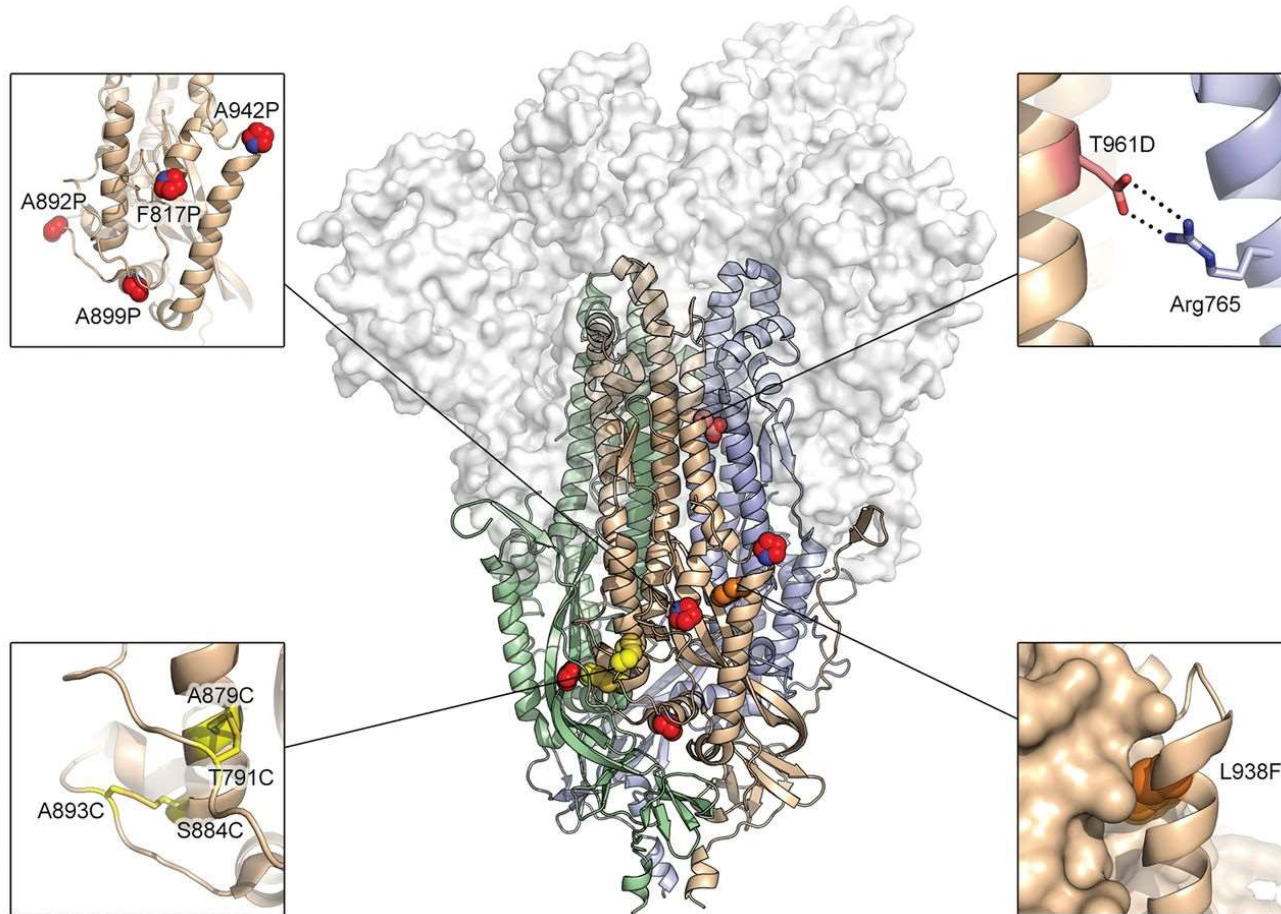
ML Model Predictions of Stabilizing RSV F Cavity-Filling Substitutions



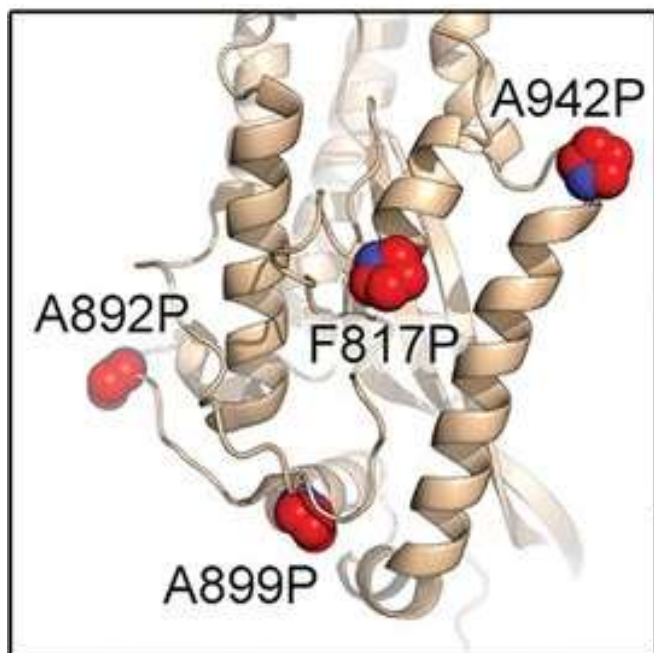
	S190F	V207L
Stability Oracle ($\Delta\Delta G$)	-1.0	-0.1
Stability Fold ($\Delta\Delta G$)	0.4	0.4
Prostata-IFML ($\Delta\Delta G$)	0.2	0.0
MutComputeX (Log Probability)	1.4	-0.4
ProteinMPNN (Log Probability)	0.7	0.0

$\Delta\Delta G < 0$ and Log Probability > 0 are predicted to be beneficial

Exemplary Substitutions for SARS-CoV-2 Spike (S) Stabilization



ML Model Predictions of Stabilizing SARS-CoV-2 S Proline Substitutions

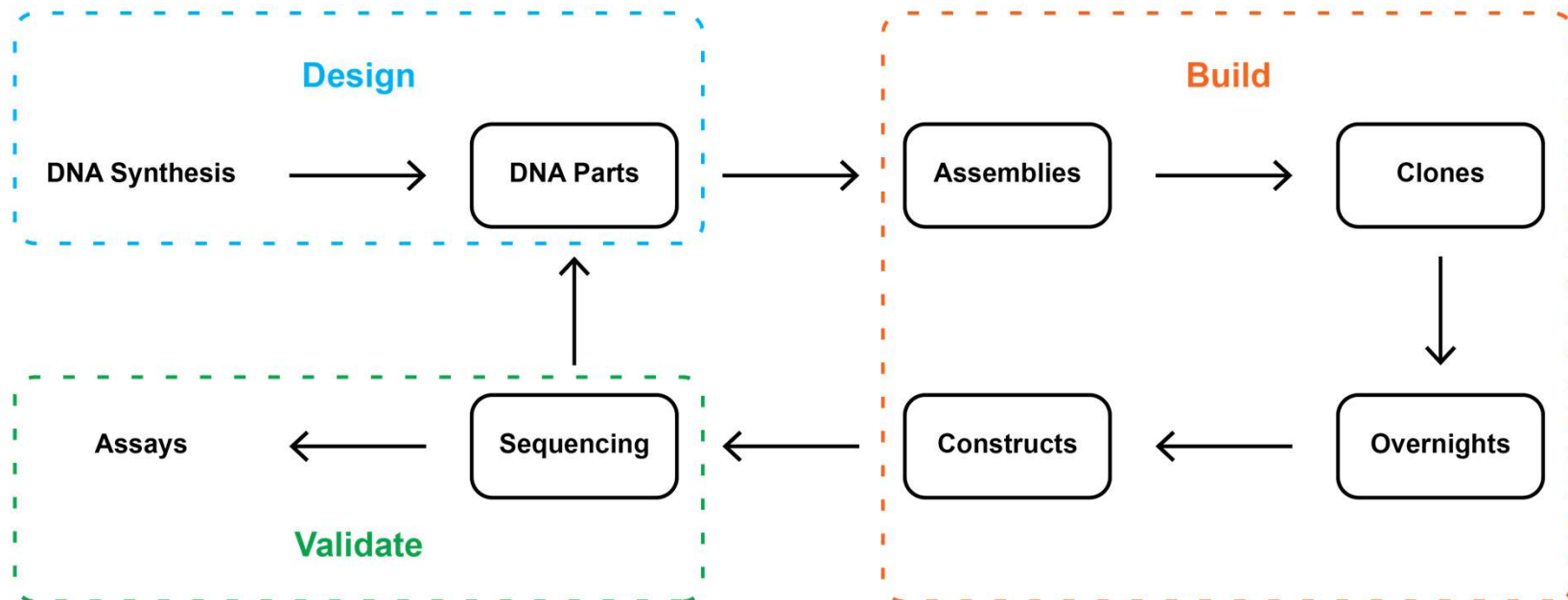


	F817P	A892P	A899P	A942P
Stability Oracle ($\Delta\Delta G$)	-0.1	-0.9	1.6	0.1
Stability Fold ($\Delta\Delta G$)	1.0	0.0	0.8	1.3
Prostata-IFML ($\Delta\Delta G$)	1.1	0.8	1.0	1.7
MutComputeX (Log Probability)	0.9	2.3	0.4	-0.1
ProteinMPNN (Log Probability)	1.6	-0.1	-0.6	1.0

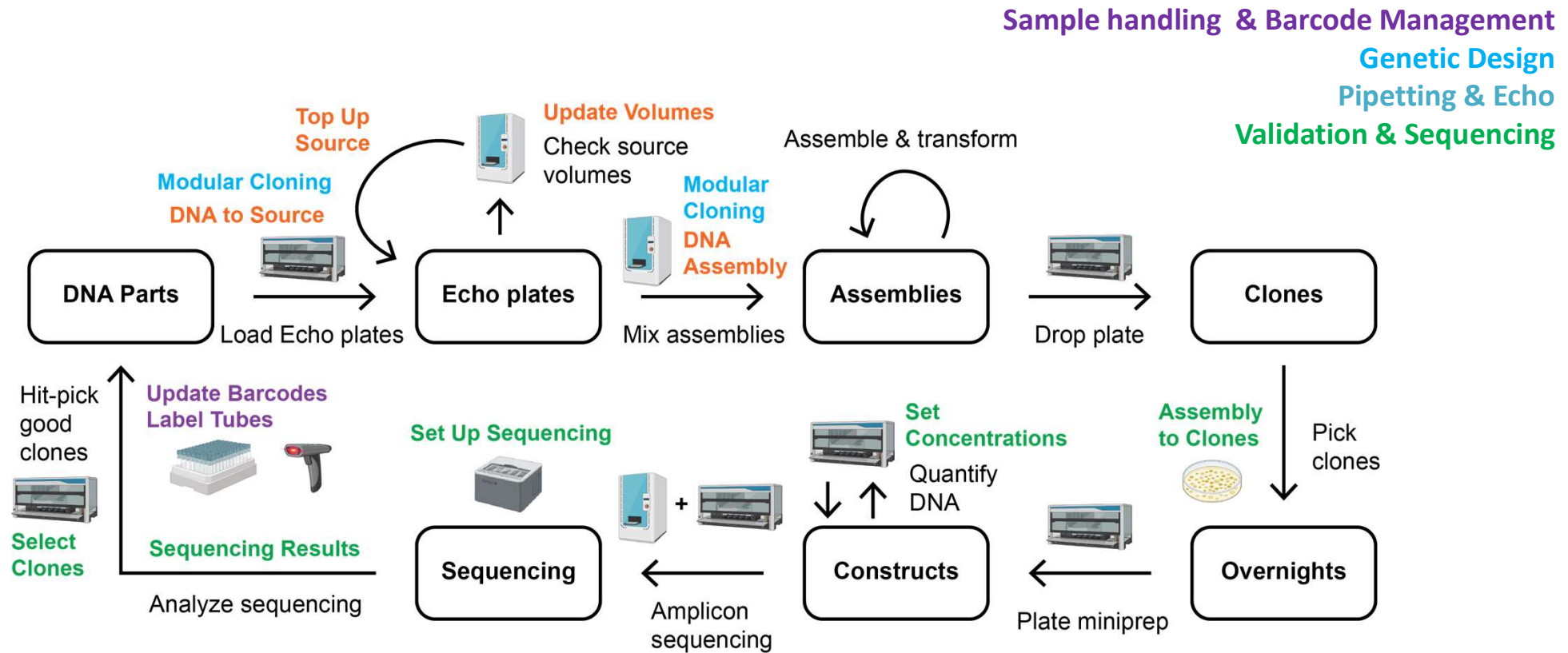
$\Delta\Delta G < 0$ and Log Probability > 0 are predicted to be beneficial

Synthetic Biology for Antigen Engineering

High-throughput synthetic biology accelerates antigen engineering by enabling rapid design-build-validate cycles for many new protein designs



Scripts are Necessary for High-throughput Synthetic Biology



Jimmy Gollihar
Houston Methodist

High-throughput Variant Screening via Flow Cytometry

- Screened 10 proline substitutions and 8 disulfide substitutions for binding to 26 antibodies in a few hours
- Heat-shocked the cells to induce conformational change and assess retention of antibody binding

Name	mAb	prolines										L4		L6		disulfides										
10.4B	1	973.03	289.88	256.53	168.71	345.04	338.79	440.5	297.47	254.97	1061.5	370.37	77.94	85.48	546.06	272.53	934.2	980.95	1343.91	1323.75	649.89					
12.1F	2	3587.36	987.53	781.57	496.72	1000.08	1027.92	1674.35	1109.8	917.79	2137.7	1460.93	87.52	97.03	2321.55	1544.67	1019.6	3487.78	3697.8	3521.91	2177.84					
18.5C	3	313.17	187.09	149.91	142.29	191.11	233.55	211.72	181.43	104.17	359.13	204.85	87.03	86.17	180.18	225.5	179.55	799.69	451.84	322.4	269.25					
18.5C-M30	4	1461.93	557.68	496.72	614.75	627.91	1309.01	812.56	921.26	136.48	1208.26	719.11	104.17	98.61	789.39	674.2	578.37	1886.22	2009.97	1537.99	632.98					
19.7E	5	2627.64	1083.98	761.62	637.94	1122.38	1192.04	1603.12	1261.92	837.59	1936.78	1467.34	84.53	86.78	2334.13	1847.71	1857.82	3226.6	3393.49	3295.73	1918.38					
25.10C	7	3925.26	1400.1	1023.76	784.06	1506.93	1669.05	2469.95	1704.2	1276.62	2835.21	2251.39	83.44	81.53	3283.35	2663.4	3388.94	4311.92	6242.23	5965.83	3693.02					
25.6A	8	402.88	209.1	174.15	155.94	207.61	262.67	234.36	210.1	126.15	261.7	197.87	89.44	83.81	263.91	221.77	192.58	681.69	536.27	454.66	313.17					
36.1F	9	1186.07	503.84	396.06	325.46	571.89	454.66	646.72	403.44	380.54	809.32	558.25	106.5	96.22	697.34	585.67	740.23	2288.48	2878.22	3359.41	1695.01					
36.9F	10	106.31	98.97	97.45	75.46	112.12	153.38	109.28	95.65	92.99	97.63	99.54	87.16	90.87	104.54	103.34	86.61	180.39	132.17	125.05	126.57					
37.2D	11	995.01	434.98	352.58	316.38	442.86	566.76	644.19	501.26	304.88	1071.07	482.79	93.95	85.39	666.76	594.09	551.84	1819.17	2036.04	1293.24	953.11					
37.2G	12	196.34	144.48	105.48	114.59	163.89	187.44	140.49	139.42	94.92	200.72	138.47	78.11	90.58	137.77	148.85	135.21	396.79	298.16	205.72	209.56					
37.7H	13	818.81	382.95	273.25	282.63	445.03	535.81	539.67	533.2	85.29	703.67	444.02	89.45	88.02	688.05	514.01	581.39	1365.59	2062.7	1315.51	883.08					
8.11G	14	943.88	365.61	292.45	255.53	387.69	370.26	482.79	360.47	293.8	567.09	375.49	85.75	80.77	507.76	442.61	526.15	1227.22	1206.12	1607.14	799.69					
8.9F	15	1158.68	243.47	164.48	123.46	296.07	291.46	363.83	357.17	184.01	349.32	310.25	82	92.71	845.03	451.14	1178.3	1291.24	1576.14	1974.06	522.9					
9.8A	16	703.67	271.82	245.38	204.6	260.26	329.28	364.13	327.31	146.71	601.77	320.66	77.42	92.46	418.97	348.37	258.56	911.75	1342.84	580.37	602					
NE13	17	200.88	121.35	115.19	106.14	137.56	152.69	146.71	129.33	96.19	160.76	147.21	82	83.03	136.77	155.94	140.37	239.52	286.6	223.5	174.82					
18.5D	18	235.74	215.02	212.09	147.08	193.24	221.52	264.35	205.6	236.52	278.6	237.84	200.36	248.14	230.63	275.6	283.57	331.01	329.26	329.89	329.93					
LAV401	19	207.84	98.16	104.17	74.32	111.85	106.99	122.51	111.76	101.96	125.73	109.75	76.9	88.02	117.74	111.5	83.36	202.57	351.07	365.9	263.5					
10.4B-U	20	3981.07	5524	4457.89	2658.26	2770.14	3354.57	4707.58	3493.44	4939.06	5401.99	5489.44	5844.94	7877.22	4763.36	7376.35	7094.59	5159.68	6515.21	6185.11	8330.17					
12.1F-pdb	21	2322.9	687.82	555.43	396.35	775.81	765.31	1268.18	894.72	672.11	1509.28	1041.74	81.11	83.2	1839.46	1196.01	928.48	3094.72	3957.64	3566.68	2293.34					
18.5C-pdb	22	114.69	200.11	159.54	158.73	223.61	252.54	213.36	204.67	95.51	395.85	186.57	83.68	88.56	204.25	216.61	185.98	502.82	502.41	360.56	316.81					
25.10C-FNQi	24	4508.66	1579.96	1283.22	766.94	2013.38	1781.65	2766.58	1873.28	1301.13	2947.19	2059.48	73.64	77.3	3240.54	2590.72	3382.21	5262.07	6293.92	6372.83	3828.47					
36.1F-pdb	25	1557.43	684.92	527.92	393.15	787.03	725.88	1018.56	661.04	504.64	1098.5	781.57	121.98	134.89	990.53	951.09	918.18	2648	3510.43	3450.23	1986.66					
8.9F-pdb	26	505.27	176.75	124.53	109.28	217.02	212.81	263.71	263.91	121.85	215.81	186.3	74.09	92.91	477.35	250.27	802.09	700.55	893.82	958.34	338.48					
Name	mAb	prolines										L4		L6		disulfides										
10.4B	1	2.63	0.78	0.69	0.46	0.93	0.91	1.19	0.80	0.69	2.87	1.00	0.21	0.23	1.47	0.74	2.52	2.65	3.63	3.57	1.75					
12.1F	2	2.46	0.68	0.53	0.34	0.68	0.70	1.15	0.76	0.63	1.46	1.00	0.06	0.07	1.59	1.06	0.70	2.39	2.53	2.41	1.49					
18.5C	3	1.53	0.91	0.73	0.69	0.93	1.14	1.03	0.89	0.51	1.75	1.00	0.42	0.42	0.88	1.10	0.88	3.90	2.21	1.57	1.31					
18.5C-M30	4	2.03	0.78	0.69	0.85	0.87	1.82	1.13	1.28	0.19	1.68	1.00	0.14	0.14	1.10	0.94	0.80	2.62	2.80	2.14	0.88					
19.7E	5	1.79	0.74	0.52	0.43	0.76	0.81	1.09	0.86	0.57	1.32	1.00	0.06	0.06	1.59	1.26	1.27	2.20	2.31	2.25	1.31					
25.10C	7	1.74	0.62	0.45	0.35	0.67	0.74	1.10	0.76	0.57	1.26	1.00	0.04	0.04	1.46	1.18	1.51	1.92	2.77	2.65	1.64					
25.6A	8	2.04	1.06	0.88	0.79	1.05	1.33	1.18	1.06	0.64	1.32	1.00	0.45	0.42	1.33	1.12	0.97	3.45	2.71	2.30	1.58					
36.1F	9	2.12	0.90	0.71	0.58	1.02	0.81	1.16	0.72	0.68	1.45	1.00	0.19	0.17	1.25	1.05	1.33	4.10	5.16	6.02	3.04					
36.9F	10	1.07	0.99	0.98	0.76	1.13	1.54	1.10	0.96	0.93	0.98	1.00	0.88	0.91	1.05	1.04	0.87	1.81	1.33	1.26	1.27					
37.2D	11	2.06	0.90	0.73	0.66	0.92	1.17	1.33	1.04	0.63	2.22	1.00	0.19	0.18	1.38	1.23	1.14	3.77	4.22	2.68	1.97					
37.2G	12	1.42	1.04	0.76	0.83	1.18	1.35	1.01	1.01	0.69	1.45	1.00	0.56	0.65	0.99	1.07	0.98	2.87	2.15	1.49	1.51					
37.7H	13	1.84	0.86	0.62	0.64	1.00	1.21	1.22	1.20	0.19	1.58	1.00	0.20	0.20	1.55	1.16	1.31	3.08	4.65	2.96	1.99					
8.11G	14	2.51	0.97	0.78	0.68	1.03	0.99	1.29	0.96	0.78	1.51	1.00	0.23	0.22	1.35	1.18	1.40	3.27	3.21	4.28	2.13					
8.9F	15	3.73	0.78	0.53	0.40	0.95	0.94	1.17	1.15	0.59	1.13	1.00	0.26	0.30	2.72	1.45	3.80	4.16	5.08	6.36	1.69					
9.8A	16	2.19	0.85	0.77	0.64	0.81	1.03	1.14	1.02	0.46	1.88	1.00	0.24	0.29	1.31	1.09	0.81	2.84	4.19	1.81	1.88					
NE13	17	1.36	0.82	0.78	0.72	0.93	1.04	1.00	0.88	0.65	1.09	1.00	0.56	0.56	0.93	1.06	0.95	1.63	1.95	1.52	1.19					
18.5D	18	0.99	0.90	0.89	0.62	0.81	0.93	1.11	0.86	0.99	1.17	1.00	0.84	1.04	0.97	1.16	1.19	1.39	1.38	1.39	1.39					
LAV401	19	1.89	0.89	0.95	0.68	1.02	0.97	1.12	1.02	0.93	1.15	1.00	0.70	0.80	1.07	1.02	0.76	1.85	3.20	3.33	2.40					
10.4B-U	20	0.73	1.01	0.81	0.48	0.50	0.61	0.86	0.64	0.90	0.98	1.00	1.06	1.43	0.87	1.34	1.29	0.94	1.19	1.13	1.52					
12.1F-pdb	21	2.23	0.66	0.53	0.38	0.74	0.73	1.22	0.86	0.65	1.45	1.00	0.08	0.08	1.77	1.15	0.89	2.97	3.80	3.42	2.20					
18.5C-pdb	22	1.69	1.07	0.86	0.85	1.20	1.35	1.14	1.10	0.51	2.12	1.00	0.45	0.47	1.09	1.16	1.00	2.70	2.69	1.93	1.70					
25.10C-FNQi	24	2.19	0.77	0.62	0.37	0.98	0.87	1.34	0.91	0.63	1.43	1.00	0.04	0.04	1.57	1.26	1.64	2.56	3.06	3.09	1.86					
36.1F-pdb	25	1.99	0.88	0.68	0.50	1.01	0.93	1.30	0.85	0.65	1.41	1.00	0.16	0.17	1.27	1.22	1.17	3.39	4.49	4.41	2.54					
8.9F-pdb	26	2.71	0.95	0.67	0.59	1.16	1.14	1.42	1.42	0.65	1.16	1.00	0.40	0.50	2.56	1.34	4.31	3.76	4.80	5.14	1.82					

Summary

Summary

- New advances in cryo-EM have enabled higher resolution and higher throughput than ever before
- Techniques such as EMPEM provide valuable insights into polyclonal immune responses to vaccination and infection
- AI/ML combined with high-throughput screening is allowing accelerated development of vaccine antigens for important human pathogens

Acknowledgements

McLellan Laboratory

Jory Goldsmith

Ching-Lin Hsieh

Ling Zhou

Nianshuang Wang

Daniel Wrapp

Patrick Byrne

Christy Hjorth

Nicole Johnson

Ryan McCool

Cory Acreman

Institute for Machine Learning

Adam Klivans

Danny Diaz

Houston Methodist

Jimmy Gollihar